

## **Coronal Loops Heated by MHD Turbulence: I. A Model of Isobaric Quiet Sun Loops with Constant Cross-sections**

Jongchul Chae<sup>1,2</sup>, Arthur I. Poland<sup>3</sup> and Markus J. Aschwanden<sup>4</sup>

### **ABSTRACT**

Several recent papers have presented new observational results indicating that many coronal loops in active regions are nearly isothermal. It is expected that quiet Sun loops may have similar thermal structures, since quiet Sun differential emission measures look similar to those in active regions. In the quiet Sun, it has been well-known from observations that the non-thermal velocity inferred from the excess broadening of a line over thermal broadening reaches a peak of about  $30 \text{ km s}^{-1}$  around  $3 \times 10^5 \text{ K}$ , and then decreases with temperature, having a value of about  $20 \text{ km s}^{-1}$  at  $1 \times 10^6 \text{ K}$ . In the present work, we make the assumption that the observed non-thermal velocities are a manifestation of magnetohydrodynamic (MHD) turbulence, and present a model of static, isobaric coronal loops heated by turbulence. Instead of solving the MHD equations, we adopt simple energy spectra in MHD turbulence and infer the heating rate as a function of temperature from the observed non-thermal velocities. By solving the steady-state energy equation of a loop in which temperature monotonically increases with height, we obtained the following results: (1) The heating rate is predominantly near the footpoints, and decreases with the loop arc length. (2) There is a critical temperature above which the loop can not be maintained in a steady state. (3) The loop is denser, and is more isothermal than uniformly heated loops, being compatible with recent observations. (4) The theoretical differential emission measures are in good agreement with the empirical values at temperatures above  $10^5 \text{ K}$ . Below this temperature we still have a large discrepancy. (5) It is possible to explain the observed strong correlation between intensity and non-thermal velocity of a spectral line in the quiet Sun. Our results support the idea that quasi-statically driven magnetohydrodynamic turbulence of the direct current (DC) type in the stratified medium (transition region and corona) is a viable mechanism for coronal heating.

---

<sup>1</sup>Department of Astronomy and Space Science, Chungnam National University, Daejeon 305-764, Korea ( chae@cnu.ac.kr )

<sup>2</sup>Big Bear Solar Observatory, NJIT, 40386 North Shore Lane, Big Bear City, CA 92314, USA

<sup>3</sup>Solar Physics Branch, Laboratory for Astronomy and Solar Physics, NASA/Goddard Space Flight Center, Greenbelt, MD 20771

<sup>4</sup>Lockheed Martin Advanced Technology Center, Solar & Astrophysics Laboratory, Department L9-41, Building 252, 3251 Hanover Street, Palo Alto, CA 94304

## 1. INTRODUCTION

One of the major findings of recent solar observations is that the solar transition region and corona display a great diversity of dynamic features and transient brightenings spanning nearly all observable sizes and time scales, and probably extending far below the resolution limit of the present observing capabilities (for a review of this, see Aschwanden, Poland & Rabin 2001). This finding gives the impression that the solar transition region and corona may be in a turbulent state in which physical processes at different scales are intimately related. Since the dynamics of the solar upper atmosphere is dominated by magnetic fields, it is likely that the turbulence may be of magnetohydrodynamic (MHD) nature, not simply the traditional hydrodynamic turbulence.

Generally speaking, MHD turbulence may arise when MHD perturbations develop non-linearly. The conventional picture of MHD turbulence proposed for explaining heating of a coronal loop is as follows. Perturbations are produced near footpoints, e.g., by photospheric shuffling motion, and propagate to the upper portion of the loop. As a result, in every portion of the loop the magnetic field as well as the velocity field is disturbed and fluctuates. When the fluctuation amplitudes are big enough, the fluctuations evolve non-linearly and MHD turbulence sets in. The magnetic energy and kinetic energy contained in the fluctuations cascade down to smaller and smaller scales, and are eventually converted into heat through ohmic and viscous dissipation. If photospheric agitation takes place continuously, a steady state may be reached in which the rate of energy injected at the footpoints by photospheric shuffling motions, and the rate of energy cascading down to smaller scales, and the rate of energy dissipation, which is the heating rate, are all the same.

Recently Schrijver & Aschwanden (2002) developed a prototype of a global atmospheric, empirical model and parameterized the heating flux density passing through a loop base as a function of the base magnetic field strength, loop length, and footpoint velocity. From the comparison of the parametrization to various heating models, they found that MHD turbulence and the dissipation of current layers are the most likely candidate heating mechanisms. This conclusion further narrowed the group of the most likely heating models as chosen by Mandrini, Démoulin, & Klimchuk (2000). On the other hand, Aschwanden (2001) pointed out that the present versions of MHD turbulence models are not compatible with the recent observational finding of a coronal heating function localized near the footpoints of loops, as inferred from the near-isothermal nature of coronal loops (Aschwanden, Nightingale, & Alexander 2000; Aschwanden, Schrijver, & Alexander 2001). Because the turbulent plasma is generally modeled in a homogeneous axial magnetic field and with homogeneous electron density (Dmitruk & Gomez 1997, 1999; Heyvaerts & Priest 1992; Inverarity, Priest, & Heyvaerts 1995; Inverarity & Priest 1995) it produces uniform heating, which does not agree with the observations. Therefore, for a rigorous evaluation of the heating of the corona by MHD turbulence, it is necessary to develop a theory of MHD turbulence in a highly stratified medium, probably with a complex magnetic geometry. This is a formidable task far beyond our capabilities.

In the present work, we adopt an alternative approach to examine whether MHD turbulence is a potential candidate for the coronal heating mechanism. We combine spectroscopic observations

of the solar transition region and corona with a simple theory of MHD turbulence. Specifically we make use of non-thermal velocities determined from the excess broadening of spectral lines over thermal broadening. Chae, Schühle, & Lemaire (1998a) performed an extensive study of nonthermal velocities in the quiet Sun based on a number of spectral lines recorded by the SUMER / SOHO, and produced the dependence of non-thermal velocity on temperature from  $10^4$  K to  $10^6$  K (see Figure 1). Assuming the non-thermal motions represent velocity fluctuations associated with MHD turbulence, we determine the turbulent heating rate as a function of temperature, based on this observation, and construct a model of coronal loops that are in energy balance between turbulent heating rates, radiative losses, and thermal conduction. Then we examine the properties of model loops heated by MHD turbulence, and compare them with observations. Our results show that the non-uniform heating can reproduce the observed differential emission measures of quiet Sun loops fairly well at temperatures above  $10^{5.3}$  K, and suggest that MHD turbulence is a highly viable mechanism of coronal heating.

## 2. LOOP MODEL

Our focus is on the role of turbulent heating on the structure of coronal loops, so some simplifying assumptions will serve our purpose. We consider a loop in a steady-state, which has (1) zero bulk motion  $v(s) = 0$ , (2) constant pressure  $p(s) = \text{const}$ , and (3) constant cross-section  $A(s) = \text{const}$  or equivalently constant axial field strength  $B_o(s) = \text{const}$ . Our approach is a generalized application of the method used by Rosner et al. (1978) to the non-uniform heating. Temperature will be determined as a function of the distance  $s$  along the loop from the energy balance equation

$$\frac{dF_c}{ds} = E_H - E_R \quad (1)$$

with the conductive flux of thermal energy along the loop

$$F_c = -\kappa T^{5/2} \frac{dT}{ds}, \quad (2)$$

with  $\kappa = 1 \times 10^{-6}$  in cgs units and the radiative cooling

$$E_R = n_e^2 \Phi(T) = \frac{p^2}{4k_B^2 T^2} \Phi(T) \quad (3)$$

where  $\Phi(T)$  is the radiative loss function,  $n_e$  the electron density,  $p$  the pressure, and  $k_B = 1.38 \times 10^{-16}$  erg K<sup>-1</sup> the Boltzman constant. We used the equation of state  $p = 2n_e k_B T$  for ideal gas made up of fully ionized hydrogen. The heating rate  $E_H$  is essential in all loop models, but has remained physically unspecified so far. Rosner et al. (1978) treated it simply as a constant free parameter to be determined by the boundary conditions. In the present work, we adopt the following expression of the turbulent heating rate  $E_H$

$$E_H = \frac{\epsilon_o}{l_{in}} \frac{\rho \xi^4}{v_A} \quad (4)$$

where  $\xi$  is the non-thermal speed,  $\rho$ , mass density,  $v_A = B_o/\sqrt{4\pi\rho}$ , the Alfvén speed,  $l_{in}$ , the length scale over which energy injection occurs, and  $\epsilon_o$ , a dimensionless factor. In the Appendix, we have derived this expression, and have shown that  $\epsilon_o$  is related to the ratio of magnetic energy to kinetic energy  $q$ . In the present work, we will regard  $\epsilon_o/l_{in}$  as a free parameter to be determined by the loop model. Under the assumption of constant pressure  $p$  and constant axial magnetic field strength  $B_o$ , the heating rate is fully specified as a known function of  $T$ , if  $\xi$  is known to be a function of  $T$ . For convenience, we express the heating rate as the product of the characteristic heating rate  $E_c$  at a prescribed coronal temperature  $T_c$  (which is chosen to be  $10^6$  K without loss of generality), and the normalized heating function  $h(T)$ :

$$E_H(T) = E_c h(T) \quad (5)$$

where

$$E_c = \frac{1}{4} \left[ \frac{m_H}{k_B} \right]^{3/2} \frac{\epsilon_o}{l_{in}} \sqrt{\beta} p \frac{\xi_c^4}{T_c^{3/2}} \quad (6)$$

and

$$h(T) = \left( \frac{\xi}{\xi_c} \right)^4 \left( \frac{T}{T_c} \right)^{-3/2} \quad (7)$$

introducing the plasma parameter  $\beta \equiv 8\pi p/B_o^2$  which is also constant along the loop. Now we regard  $E_c$  itself as a constant free parameter to be determined by the loop model.

We only consider one half of a symmetric loop whose temperature monotonically increases from the footpoints to the apex, as was also considered by Rosner et al. (1978). By imposing the condition that the conductive energy flux vanishes at both the upper boundary  $T = T_m$  ( $T_m$  is the loop apex temperature) and the lower boundary  $T = T_0$ , we can derive the expression of  $F_c$  as a function of  $T$ ,  $T_m$  and  $p$

$$F_c(T) = -\sqrt{2\kappa p} [g_r(T_m)]^{1/2} \left[ \frac{g_r(T)}{g_r(T_m)} - \frac{f_h(T)}{f_h(T_m)} \right]^{1/2} \quad (8)$$

and  $E_c$  as a function of  $T_m$  and  $p$

$$E_c = \frac{g_r(T_m)}{f_h(T_m)} p^2 \quad (9)$$

with the two auxiliary functions

$$g_r(T) = \frac{1}{4k^2} \int_{T_0}^T t^{1/2} \Phi(t) dt \quad (10)$$

$$f_h(T) = \int_{T_0}^T t^{5/2} h(t) dt \quad (11)$$

where  $g_r$  and  $f_h$  represent the radiation loss and heating contributions to the thermal conductive flux  $F_c$  (first defined in Rosner et al. 1978). Examples of the heating related functions  $h(T)$  and

$f_h(T)$  are presented in Figure 2 and the radiative cooling related functions  $\Phi(T)$  and  $g_r(T)$  are in Figure 3. Note that the necessary condition for a solution to exist is

$$\frac{g_r(T)}{f_h(T)} \geq \frac{g_r(T_m)}{f_h(T_m)} \text{ for } T_0 \leq T \leq T_m. \quad (12)$$

Finally, combining Equations 2, 8, we derive the scaling relation

$$pL \equiv p [s(T_m) - s(T_0)] = \sqrt{\frac{\kappa}{2}} \frac{T_m^{7/2} \eta(T_m)}{[g_r(T_m)]^{1/2}} \quad (13)$$

and the implicit form of the temperature profile  $T(s)$  is given by

$$\frac{s(T) - s(T_0)}{L} = \frac{\eta(T)}{\eta(T_m)} \quad (14)$$

where

$$\eta(T) = \int_{T_0}^T \left( \frac{t}{T_m} \right)^{5/2} \left[ \frac{g_r(t)}{g_r(T_m)} - \frac{f_h(t)}{f_h(T_m)} \right]^{-1/2} \frac{dt}{T_m}. \quad (15)$$

Note that given prescribed  $\Phi(T)$  and  $h(T)$  (where  $h(T)$  is derived from the observed excess line broadenings, or equivalently  $g_r(T)$  and  $f_h(T)$ ), the loop is fully specified by the pair of two independent parameters  $p$  and  $T_m$ .

A quantity that can be directly compared with observations is the differential emission measure of a loop given by

$$Q_{\text{loop}}(T) = n_e^2 \left| \frac{ds}{dT} \right| = \frac{\sqrt{\kappa}}{4\sqrt{2}k^2} p [g_r(T_m)]^{-1/2} T^{1/2} \left[ \frac{g_r(T)}{g_r(T_m)} - \frac{f_h(T)}{f_h(T_m)} \right]^{-1/2}. \quad (16)$$

Note for given  $T$  and  $T_m$ ,  $Q_{\text{loop}}$  is proportional to  $p$ . This means that the intensity of a spectral line is proportional to  $n_e$  if  $T_m$  is kept fixed, even though the volumetric radiative loss rate is proportional to  $n_e^2$ . This information is helpful in relating the observed intensity of a spectral line

emitted by loops to the loop parameter  $n_e$  or  $p$ , and the relevant heating rate  $E_c$ .

### 3. RESULTS

#### 3.1. Uniform Heating Versus Non-uniform Heating

We will compare two kinds of loops heated by MHD turbulence. The first are loops uniformly heated by MHD turbulence. The model of uniformly heated loops was extensively studied by Rosner et al. (1978), even though they did not mention MHD turbulence as a possible origin of heating. For MHD turbulence heating to be uniform, it is required that  $h(T) = 1$  or

$$\xi = \xi_c \left( \frac{T}{T_c} \right)^{3/8}. \quad (17)$$

indicating that  $\xi$  should increase with  $T$ . Figure 1, however, shows that  $\xi$  measured in the quiet Sun has a peak around  $2.5 \times 10^5$  K and decreases with  $T$  at higher temperatures. This temperature dependence of quiet Sun average non-thermal velocities is fairly approximated by the analytical fit:

$$\xi = 27.7 - 15.56(\log T - 5.36)^2 \quad \text{km s}^{-1}. \quad (18)$$

This behavior is much different from what is expected in uniformly heated loops. We use the observed  $\xi$  as an input and construct the second kind of loops that are non-uniformly heated and appear to better model real loops in the quiet Sun than uniformly heated loops.

Center-to-limb measurements of line widths (Mariska et al. 1978; Chae et al. 1998a; Doyle, Teriaca, & Banerjee 2000) ) have indicated that the non-thermal velocities are more or less isotropic at all temperatures. This finding might raise a question on the validity of the MHD turbulence interpretation of non-thermal velocities, for even turbulent motion may tend to be parallel to the magnetic field in a low  $\beta$  plasma. According to the recent theoretical study done by Cho & Vishniac (2000), however, the anisotropy of MHD turbulence is weaker in larger eddies. Since the measured non-thermal motions are dominated by large velocity eddies of MHD turbulence, they may turn out to be more or less isotropic, even if small scale eddies may still have anisotropy.

Figure 2 shows a comparison of the functions  $h$  and  $f_h$  in the uniformly and non-uniformly heated loops. We have set  $T_o = 2 \times 10^4$  K. We find from the figure that the non-uniform quiet-Sun heating rate is peaked around  $6 \times 10^4$  K, and decreases with  $T$  in the upper transition region and corona. The relevant function  $f_h$  increases rapidly in the lower transition region, but becomes saturated at coronal temperatures.

### 3.2. Existence of Critical Temperature

Figure 3 shows the Raymond radiative loss function  $\Phi(T)$  given in Rosner et al. (1978) and Mariska (1992), and the associated auxiliary function  $g_r(T)$ . We use the Raymond radiative loss to simplify comparison with Rosner et al. (1978). We note that it is assumed that the radiative loss is optically thin.

The ratio of  $g_r(T)$  to  $f_h(T)$  has been plotted in Figure 4 in the two cases, respectively. In the case of uniform heating, the function  $g_r/f_h$  decreases monotonically with  $T$  over the whole range of temperature. Thus, the condition that is imposed on  $g_r/f_h$  for a solution to exist (equation 12) is always fulfilled for any value of  $T_m$ . This means that there is no limitation in choosing  $T_m$  for the case of uniform heating. In contrast, the function  $g_r/f_h$  in the case of quiet Sun heating reaches a minimum at a specific temperature  $1.24 \times 10^6$  K, and then increases with  $T$  at higher temperatures. Because of this behavior, condition 12 is fulfilled only when

$$T_m \leq 1.24 \times 10^6 \text{ K}. \quad (19)$$

This limitation results from the fact that hotter loops can not be maintained in a steady state, since at hotter temperatures the heating rate is too low to balance the radiative cooling rate. Our model

thus predicts that quiet Sun loops should be cool, being consistent with the observational studies of differential emission measure in the quiet Sun (e.g., Raymond & Doyle 1981) which indicate that most quiet sun coronal loops are cooler than  $2.0 \times 10^6$  K.

### 3.3. Scaling Relations for $E_c$

The scaling relation for the heating rate  $E_c$  for a given  $p$  and  $T_m$  has been specified by Equation 9 and is plotted in Figure 4. Note that the dependence of  $E_c$  on  $T_m$  in the non-uniform quiet Sun heating is less strong than in the uniform heating. Particularly, for  $T_m$  near the critical temperature  $1.24 \times 10^6$  K, we can approximate the quiet Sun heating rate as

$$E_c \approx 2 \times 10^{-3} p^2, \quad (20)$$

which can be combined with Equation 6 to yield

$$p \approx 1.7 \times 10^{-19} \frac{\epsilon_o}{l_{in}} \sqrt{\beta} \xi_c^4. \quad (21)$$

This equation is physically important since it connects MHD turbulence parameters ( $\epsilon_o$ ,  $l_{in}$  and  $\beta$ ) and an observable parameter  $\xi_c$  to a loop parameter  $p$ . The physical implication of this equation will be discussed in the next section in relation to the nature of MHD turbulence.

### 3.4. Scaling Relations for $L$

Figure 5 shows the scaling relations for  $pL$  based on Equation 13 in the two cases. Note that the scaling relation in uniform heating is well approximated by Rosner et al.'s analytical scaling law, which was obtained by assuming simple radiative loss  $\Phi(T) = 10^{-18.81} T^{-1/2}$ . The slight difference is simply due to the fact that the RTV scaling law is based upon a simple power law approximation for the radiative loss rate, while our model uses the original function without approximation.

The scaling relation in non-uniform quiet Sun heating is obtained only at temperatures below the critical temperature  $1.24 \times 10^6$  K. Note that the non-uniformly heated loops with  $T_m \approx 1.24 \times 10^6$  K have  $pL$  larger than uniformly heated loops having the same  $T_m$ , by a factor of up to 10. Namely, for a given  $T_m$  the non-uniformly heated loops are either denser or longer by the same factor. Equivalently, for a given  $pL$  the non-uniformly heated loops are cooler than uniformly heated loops.

Of specific interest are non-uniformly heated quiet Sun loops having coronal temperatures at the apex  $T_m \sim 10^6$  K. For these loops, the scaling relation is roughly given by

$$pL \approx \left( \frac{T_m}{1.6 \times 10^4} \right)^5. \quad (22)$$

According to this scaling relation, when a typical quiet Sun pressure  $p = 0.2 \text{ erg cm}^{-3}$  (Mariska 1992) is used, loops with the apex temperatures  $T_m = 0.8 - 1.2 \times 10^6 \text{ K}$  would have half-lengths  $L = 16 - 120 \text{ Mm}$ . It is interesting that a large range of loop lengths (varying by a factor of up to an order of magnitude) fall in a very narrow range of temperature (varying by a few hundred thousand degrees). This theoretical characteristic appears to be compatible with the observations. It is inferred, from the observed differential emission measures of the quiet Sun determined by different authors (see Figure 9), that temperatures of quiet Sun loops are mostly lower than  $2 \times 10^6 \text{ K}$ , and the most probable values are in the range  $0.8 - 1.4 \times 10^6 \text{ K}$ .

### 3.5. Quiet Sun Heating Rates as Functions of Arc length

Up to this point, the normalized rates of heating by MHD turbulence  $h$  have been specified as functions of temperature, as shown in Equations 21 and 18. Once the energy balance equation is solved, we can relate  $T$  to  $s$ , so it is possible to rewrite  $h$  as a function of  $s$ . Figure 6 presents the normalized turbulent heating rate as a function of arc length  $s$  along the loop in three different cases of  $T_m$ . Obviously  $h$  decreases with  $s$  meaning that more energy is deposited near the footpoints than at the apex. Furthermore, we find from the figure that the normalized heating rate is fairly well approximated by a power law

$$h(s) \approx 3.0 \times 10^5 (ps)^{-0.63} \quad (23)$$

in all three cases of  $T_m$ , except near the loop tops where the heating rate becomes flatter over  $s$ . By combining this equation with Equation 20, we obtain  $E_H$  as a function of  $p$  and  $s$

$$E_H(p, s) \approx 6.0 \times 10^2 p^{1.37} s^{-0.63}. \quad (24)$$

This function may be used to derive the flux of mechanical energy for heating half of the loop  $F_H$

$$F_H \equiv \int_{s_o}^L E_H(p, s) ds \approx 9.6 \times 10^5 \left( \frac{p}{0.2 \text{ dyn cm}^{-2}} \right)^{1.37} \left( \frac{L}{120 \text{ Mm}} \right)^{0.37}. \quad (25)$$

It should be emphasized that the functional form of the heating function  $E_H(s)$  is an output of our models, obtained by combining an MHD turbulence theory, energy balance, and observations. The obtained form of  $E_H(s)$  clearly indicates that heating decreases with  $s$ . But the specific  $s$ -dependence of our  $E_H$  is different from the exponential form  $E_H = E_o \exp(-s/s_H)$  first introduced by Serio et al. (1981) in order to parameterize heating functions that decrease with  $s$ . The difference may be partly attributed to our simplifying assumption that pressure is constant along the loop. If a realistic exponential function were used to describe  $p$  instead of assuming the pressure constancy, the heating function would tend to be like an exponential function as used by Serio et al. We plan to investigate this aspect in subsequent work.

### 3.6. Temperature Profiles

Figure 7 compares the spatial variation of temperature along the loop in several cases of apex temperature  $T_m$ . For comparison we have plotted the RTV analytical solution  $(s - s_o)/L = \beta((T/T_m)^{5/2}; 6/5, 1/2)$  where  $\beta$  is the normalized incomplete beta function. Note this solution was first derived by Martens (1981) and Kuin & Martens (1982), and the original RTV solution presented in the appendices of Rosner et al. (1978) is not exact. As expected, the temperature profile of a loop uniformly heated by MHD turbulence almost matches the RTV solution. The slight difference is simply due to the fact that the RTV solution uses a simple power law approximation for radiative loss rate, while our model uses the original function without approximation. The figure, moreover, shows that the temperature profile of a non-uniformly heated loop with  $T_m = 0.5 \times 10^6$  K becomes similar to the RTV solution. This is because the temperatures in such a loop are limited to a narrow range so that even the non-uniform heating rate effectively becomes more or less uniform along the loop. As  $T_m$  approaches the critical temperature above which steady-state loops can not be maintained, however, the temperature profile of the non-uniformly heated loop deviates more and more from the RTV solution.

Temperature inside a non-uniformly heated loop with  $T_m \approx 1.24 \times 10^6$  K rapidly increases with  $s$  near the footpoint and then very slowly increase with  $s$  at the higher portions. As a consequence, the coronal portion of the loop ( e.g. with  $s/L > 0.2$ ) appears more or less isothermal. From recent studies (Aschwanden et al. 2000, 2001), it is well known that this kind of temperature profile results from depositing more energy near the footpoint.

Aschwanden & Schrijver (2002, AS) found that the temperature profile of a hydrostatic loop with an energy deposit rate of the form  $E_H = E_o \exp(-s/s_H)$  with a heating scale length  $s_H$  is analytically well fit by a generalized elliptical function of the form

$$\frac{T}{T_m} = [1 - (1 - s/L)^a ]^b \quad (26)$$

with  $a = 2.098 + 0.258(L/s_H)^{1.565}$  and  $b = 0.320 - 0.009(L/s_H)^{0.877}$  in the case  $T_m \sim 10^6$  K. The figure presents an AS solution with a choice of  $L/s_H = 4$ . It can be seen from the figure that this AS solution is similar to the profile of our model loop with  $T_m = 1.2 \times 10^6$  K. The discrepancies may be partly attributed to our assumption of pressure constancy. But for this minor difference, the proximity of the two solutions is good, which implies that the turbulent heating function may be approximated as an exponential function with  $s_H = L/4$ . It was already shown that  $L = 120$  Mm for a loop with  $T_m = 1.2 \times 10^6$  K if  $p = 0.2$  dyn cm<sup>-2</sup>. Therefore, we obtain  $s_H = 30$  Mm. Note if the pressure constancy were relaxed, the heating rate would decrease faster with  $s$  due to pressure stratification and the corresponding  $s_H$  would become smaller than 30 Mm.

### 3.7. Energy Balance

Figure 8 shows the spatial variation of the ratio of radiative cooling rate to heating rate,  $E_R/E_H$ . In uniformly heated loops conductive cooling dominates in the upper portion of the loop ( $E_R/E_H \ll 1$ ), and radiative cooling dominates in the lower portion ( $E_R/E_H \gg 1$ ).

In contrast in the non-uniformly heated loop, radiative cooling is important at all portions of the loop ( $E_R/E_H > 0.5$ ). In particular, in the upper portion, heating is almost balanced by radiative cooling ( $E_R/E_H \sim 1$ ). As a consequence conduction plays a minor role, thus explaining why the loop is nearly isothermal in the upper portion.

### 3.8. Differential Emission Measure

In the quiet Sun, it is hard to find spatially resolved quiet Sun loops, so the direct observational information on the structure of quiet Sun loops is quite limited. Instead, one may infer the structure of quiet Sun loops indirectly from the observed differential emission measures. The differential emission measure characterizes the UV and EUV emission from an ensemble of loops as a function of temperature. Observed differential emission measure in units of  $\text{cm}^{-5} \text{K}^{-1}$  may be written as

$$Q(T) = \frac{\int_{V_1} \rho(t) dV}{S \Delta T} \quad (27)$$

where  $S$  is the area of the observed region on the plane perpendicular to the line of sight,  $n_e$ , electron density, and  $V_1$  a volume in which temperature  $t$  satisfies  $|\log t - \log T| < a$ , and  $\Delta T = (\log(1+a) - \log(1-a))T$ . The numeric value  $a$  is commonly set to 0.15.

Suppose the volume is occupied by  $N$  identical loops of half-length  $L$ , maximum temperature  $T_m$  and constant cross-sectional area  $A$ . Then, the observed differential emission measure may be expressed as

$$Q(T) = \frac{\int_{T_1}^{T_2} \rho(t) 2NA \frac{ds}{dT} dt}{S \Delta T} = \frac{\int_{T_1}^{T_2} f Q_{\text{loop}}(t) dt}{\Delta T} \quad (28)$$

where  $T_1 = \text{Max}(0.71T, T_o)$  and  $T_2 = \text{Min}(1.41T, T_m)$ , and the effective filling factor of the ensemble of loops  $f = 2NA/S$ . Note  $Q$  results from smoothing  $Q_{\text{loop}}$  over  $T$ . As a consequence,  $Q$  does not have a singularity at  $T_m$  even if  $Q_{\text{loop}}$  does.

Figure 9 shows several quiet Sun DEMs reported by different authors. All the DEMs are qualitatively similar in that each has a local minimum at a transition region temperature and a local maximum at a coronal temperature. There is a good agreement in the shapes of the quiet Sun average DEMs of Raymond & Doyle (1981), the DEM of Griffiths et al. (2000) obtained for an enhanced network region with  $P_e = 0.25 \text{ dyn cm}^{-2}$ , and the normal network DEM of O’Shea et al. (2000). All of the DEMs have peaks around  $1.2 \times 10^6 \text{ K}$ , which is coincident with the critical temperature of the turbulently heated loops. Note that the plotted DEM of O’Shea et al. (2000) has been multiplied by a factor of  $10^{0.2}$  so as to match that of Raymond & Doyle (1981). The

logarithmic difference of 0.2 may represent the region to region variation of the DEM in the quiet Sun. The DEM of Mason et al. (1997) looks different from others. We do not know why these DEMs are significantly different from others.

For comparison with our models, the two theoretical DEMs of a uniformly heated loop and a non-uniformly heated loop were calculated, respectively, using Equations 16 and 28. We have chosen  $T_m = 1.2 \times 10^6$  for the two loops and a value of  $\log fp = -1.3$  which reasonably matches the absolute scale of the empirical DEM of Raymond & Doyle (1981). It can be seen from Figure 9 that below  $10^{5.0}$  K the models are lower than all of the observations. From  $10^{5.0}$  to  $10^{5.4}$  K both models agree with the observations. From  $10^{5.5}$  to  $10^{5.9}$  K uniform heating is too low, except for the observations of Mason et al. while the rest of the observations agree with the non-uniform heating. Curiously just above  $10^{6.0}$  K the best agreement is with Mason et al. The observations are too scattered to support any given heating model at this point. At high temperatures either model would be acceptable. At low temperatures,  $10^{5.0}$  K, neither of the theoretical DEMs match the empirical DEMs. We suspect this may be because the optically thin approximation used in the derivation of the radiative loss function may not be fully valid at these temperatures as pointed out by McClymont & Canfield (1983). However, it may also be the result of the need to include other physical processes, such as flows, ambipolar diffusion, unresolved fine structures, etc.

## 4. DISCUSSION

### 4.1. Intensity- $\xi$ Correlation

Heating by MHD turbulence may be supported by the observation that  $\xi$  and the intensity in a spectral line are strongly correlated as shown in Figure 10. Suppose that all the loops have the same  $\xi(T)/\xi_c$  and the same  $T_m$ . Under this assumption, it is expected that all the loops have the same thermal structure  $s(T)/L$  and the loop-to-loop variation is determined by the difference in  $p$ , which is in turn due to the difference in  $\xi_c$ . Note that for given  $T$  and  $T_m$ ,  $Q_{\text{loop}}$  and line intensity is proportional to  $p$ . Then, the relation in Equation 21 predicts in a spectral line formed at a temperature  $T$  the intensity  $I$  should be proportional to  $\xi_c^4$  and hence

$$I(T) \propto \xi^4(T). \quad (29)$$

This prediction well explains the correlation of intensity and  $\xi$  of the Si IV  $\lambda$  1402 line shown in Figure 10.

### 4.2. Inhomogeneous MHD Turbulence

We have interpreted the observed non-thermal velocities as a manifestation of MHD turbulence. As a matter of fact, the non-thermal velocity varies with the line formation temperature, suggesting

that MHD turbulence in the solar transition region and corona may be inhomogeneous. This may not be surprising in view of the fact that the density and temperature of the plasma in the transition region are highly stratified. The simple energy cascade theory adopted for the present study was originally derived for homogeneous MHD turbulence. We used it to examine the effect of inhomogeneous MHD turbulence with the help of observations. Hence, strictly speaking, there is an inconsistency. But it is the most reasonable approach at present that can be used to determine the non-uniform heating as a function of temperature.

From an ideal point of view, it would be essential to develop a theory of MHD turbulence in such a highly inhomogeneous medium in a consistent way. Matthaeus et al. (1999) and Oughton et al. (2001) may be the first to implement the strong density stratification in the solar transition region and corona into the theory of MHD turbulence. They argued that the rapid increase of Alfvén speed with height implied by the rapid density decrease leads to the reflection of the upward-propagating Alfvén waves, and the collision of the low frequency upward-propagating waves and the reflected waves may drive MHD turbulence to where a nonlinear cascade results in high frequency fluctuations. This idea is attractive since it may provide a way of describing inhomogeneous MHD turbulence in a highly stratified medium. The idea was originally proposed to explain the heating of the solar corona in open field line regions, but its principle could be applied to closed field line regions with loops, too. It would be very interesting to see if the proposed mechanism reproduces the observed temperature dependence of the non-thermal velocities shown in Figure 1.

### 4.3. Turbulence Parameters

Our results may be exploited to infer some of physical parameters of MHD turbulence that may cause coronal heating. In the average quiet Sun we can take  $\xi_c = 20 \text{ km s}^{-1}$ , a typical magnetic field strength of 10 G, and a typical gas pressure of  $0.2 \text{ dyn cm}^{-2}$ , and hence  $\beta \approx 0.05$ . Then from Equation 21, we obtain  $\epsilon_o/l_{in} = 3.2 \times 10^{-7} \text{ cm}^{-1}$ . What would be the scale length  $l_{in}$  where energy injection mainly occurs? A natural choice would be either the size of granules where the excitation occurs or the width of the coronal portion of the loop where MHD turbulence develops, both of which are typically about 1 Mm. Choosing this value constrains the dimensionless parameter  $\epsilon_o \approx 32$ . Note that  $\epsilon_o$  depends on the ratio  $q$  of turbulent magnetic energy to turbulent kinetic energy (see Equation A10 in Appendix). Thus it follows  $q \approx 14$ . If we instead use a smaller value, e.g.,  $l = 10^2 \text{ km}$  to be conservative, we have  $\epsilon_o \approx 3$  and  $q \approx 5$ . In both cases, it is found that turbulent magnetic energy of MHD turbulence dominates over turbulent kinetic energy. Therefore, our results support the direct current (DC) picture that MHD turbulence is driven quasi-statically.

## 5. SUMMARY AND CONCLUSION

We have investigated the effect of heating through MHD turbulence on the structure of coronal loops. Instead of solving the MHD equations, we have adopted simple energy spectra of MHD turbulence and inferred the heating rate as a function of temperature from the observed non-thermal velocities seen in excess broadening of UV/EUV line profiles. Since both the observed non-thermal velocity and density decrease with temperature, the heating rate is also a function that decreases with temperature, which means more heating at the footpoints of loops than at their tops. The main results of modeling quiet Sun loops are as follows:

1. There is a critical temperature above which the loop can not be maintained in a steady state. The critical temperature depends on the adopted radiative loss function. When the Raymond radiative loss is used, it is  $1.24 \times 10^6$  K, which is coincident with the peak temperature of the observed differential emission measures.
2. Non-uniformly heated loops are longer and denser ( for a given apex temperature  $T_m$ ) or cooler ( for a given  $pL$ ) than uniformly heated loops.
3. The heating rate was found to decrease with  $s^{-0.63}$ .
4. The temperature profile of a non-uniformly heated loop is qualitatively similar to that of a loop with a heating function that exponentially decreases with  $s$ . Particularly, the temperature profile of a loop with  $T_m = 1.2 \times 10^6$  K is similar to the analytical solution with heating scale length  $s_H = L/4$  that was obtained by Aschwanden & Schrijver (2002).
5. The cooling of non-uniformly heated loops by radiation exceeds conductive cooling at all portions of the loop. Especially at the coronal temperature portion, radiative cooling dominates conductive cooling, and the loop appears nearly isothermal.
6. While the observed differential emission measures are too varied to make the theoretical calculations definitive, we feel that the measurements of Raymond & Doyle (1981) are best matched by the non-uniformly heated loop.

Based on these results we propose a prototype model for quiet Sun loops heated by MHD turbulence. The model is specified by two independent parameters:  $p = 0.2$  dyn cm<sup>-2</sup> and  $T_m = 1.2 \times 10^6$  K, and the relevant parameters are listed in Table 1.

In summary, our study has shown a way to estimate turbulent heating in coronal loops in the quiet Sun from the observed non-thermal line widths. Our results are consistent with: 1) the more or less isothermal structure of loops, and 2) the narrow range of apex temperatures as inferred from the observed differential emission measures. Therefore, we suggest that MHD turbulence is a highly viable mechanism for heating the solar corona.

Finally, we should mention that our model used in the present study is primitive in that it is based on many simplifying assumptions. For realistic modeling, many additional physical

factors need to be taken into account. From the point of view of loop modeling, the assumption of pressure constancy should be relaxed and the pressure stratification due to gravity should be included. It would be also necessary to investigate the effect of expansion of loop cross-section, which appears to be important at temperatures above  $10^5$  K (e.g., Chae, Yun, & Poland 1998b). At lower temperatures, flow and opacity may have to be taken into account (see Chae, Yun & Poland 1997).

This work was supported by the National Research Laboratory Project of the Korea Government (code no: M10104000059-01J000002500), and NASA (grant NAG5-10894). We thank the referee for the comments.

### A. Energy Cascade Rate in MHD Turbulence

Our strategy is to infer the rate of energy cascade — that is equal to the heating rate — from the observed non-thermal velocities based on simple theories of magnetohydrodynamic turbulence. The basic assumption is that non-thermal velocities represent random motions in MHD turbulence. Observations indicate that non-thermal velocities are isotropic (Chae et al. 1998a), so we assume turbulent velocity fluctuations are also isotropic. We denote the turbulent magnetic field by  $\mathbf{b}$  and the turbulent velocity field  $\mathbf{v}$ , respectively. Since  $\xi$  is the most probable speed of the turbulent flow along the line of sight, the turbulent kinetic energy per unit mass is given by

$$E^V \equiv \frac{1}{2} \langle |\mathbf{v}|^2 \rangle = \frac{3}{4} \xi^2. \quad (\text{A1})$$

Since the turbulent magnetic energy  $E^B \equiv |\mathbf{b}|^2/(8\pi)$  can not be determined from current observations, we introduce a free parameter  $q$ , the ratio of  $E^B$  to  $E^V$

$$q \equiv \frac{E^B}{E^V} \quad (\text{A2})$$

which is to be determined from loop models. Note that  $q$  is distinct from the plasma  $\beta$ , the ratio of kinetic energy of plasma particles (which depends on temperature) to the non-fluctuating magnetic energy (which depends on the initial magnetic field strength).

It is well known that the total (i.e. magnetic + kinetic) energy in the inertial range of MHD turbulence follows the famous Iroshnikov-Kraichnan(IK) spectrum (Biskamp 1993)

$$E(k) = E^B(k) + E^V(k) = C\sqrt{\epsilon v_A} k^{-3/2}. \quad (\text{A3})$$

Here  $k$  is the wavenumber,  $\epsilon$ , the rate of energy cascade per unit mass,  $v_A = B_o/\sqrt{4\pi\rho}$ , the local Alfvén speed, and  $C$ , a dimensionless number of order of unity, which we choose  $C = 1$ . For our application, we need a separate expression of  $E^V(k)$ . In the case of Alfvénic fluctuations (AC excitation), an equipartition holds between magnetic energy and kinetic energy at all scales

$E^V(k) = E^B(k)$  and, hence,  $q = 1$ . But this equipartition may not hold in coronal loops excited by photospheric shuffling motions, since the excitation could occur quasi-statically. Numerical studies (e.g. Dmitruk & Gómez 1999) showed that magnetic energy is significantly bigger than kinetic energy, and equipartition takes place only at very small scales. We model this behavior by introducing the difference spectrum of the form

$$E^B(k) - E^V(k) \propto k^{-\alpha}. \quad (\text{A4})$$

Recalling

$$E^B = \int_{k_o}^{\infty} E^B(k) dk \quad (\text{A5})$$

$$E^V = \int_{k_o}^{\infty} E^V(k) dk, \quad (\text{A6})$$

one can show using (A2)-A(6)

$$E^B(k) = \sqrt{\epsilon v_A} \left[ \frac{1}{2} k^{-3/2} + (\alpha - 1) \frac{(q-1)}{q+1} k_o^{\alpha-3/2} k^{-\alpha} \right] \quad (\text{A7})$$

$$E^V(k) = \sqrt{\epsilon v_A} \left[ \frac{1}{2} k^{-3/2} - (\alpha - 1) \frac{(q-1)}{q+1} k_o^{\alpha-3/2} k^{-\alpha} \right]. \quad (\text{A8})$$

Note  $k_o$  is the lowest wavenumber of the inertial regime, where excitation occurs. Combining (A1), (A6), and (A8), we obtain the heating rate per unit volume

$$E_H = \rho \epsilon = \frac{\epsilon_o \rho \xi^4}{l_{in} v_A} \quad (\text{A9})$$

with the two new parameters

$$\epsilon_o = \left[ \frac{3(q+1)}{8} \right]^2 \quad \text{and} \quad l_{in} = \frac{1}{k_o}. \quad (\text{A10})$$

Note  $\epsilon_o$  depends only on the ratio of magnetic energy to kinetic energy, and not on the specific value of the exponent  $\alpha$  introduced in (A4).

Table 1: Parameters of the prototype model of quiet Sun loops heated by MHD turbulence.

Kind	Parameter	Value
Model input parameters	Pressure $p$	$0.2 \text{ dyn cm}^{-1}$
	Loop apex temperature $T_m$	$1.2 \times 10^6 \text{ K}$
Model output parameters	Half loop length $L$	120 Mm
	Mechanical flux for heating half of a loop $F_H$	$1 \times 10^6 \text{ erg cm}^{-1} \text{ s}^{-1}$
	Filling factor $f$	0.25
	Quiet Sun average mechanical flux $fF_H$	$2.5 \times 10^5 \text{ erg cm}^{-1} \text{ s}^{-1}$
MHD turbulence parameters	Coronal non-thermal velocity $\xi_c$	$20 \text{ km s}^{-1}$
	Energy injection length $l_{in}$	1000 km or 100 km
	Magnetic to kinetic energy ratio $q$	14 or 5
AS model fit parameter	Effective heating scale length $s_H$	30 Mm

## REFERENCES

- Aschwanden, M. J., Nightingale, R. W., & Alexander, D. 2000, *ApJ*, 541, 1059
- Aschwanden, M. J., Poland, A. I., & Rabin, D. M. 2001, *ARA&A*, 39, 175
- Aschwanden, M. J., & Schrijver, C. J. 2002, *ApJ*, submitted
- Aschwanden, M. J., Schrijver, C. J., & Alexander, D. 2001, *ApJ*, 550, 1036
- Aschwanden, M. J. 2001, *ApJ*, 560, 1035
- Biskamp, D. 1993, *Nonlinear Magnetohydrodynamics*, Cambridge Monographs on Plasma Physics, Cambridge University Press, Cambridge, United Kingdom
- Chae, J., Yun, H. S., & Poland, A. I. 1997, *ApJ*, 480, 817.
- Chae, J., Schühle, U., & Lemaire, P. 1998a, *ApJ*, 505, 957
- Chae, J., Yun, H. S., & Poland, A. I. 1998b, *ApJS*, 114, 151.
- Cho, J. & Vishniac, E. T. 2000, *ApJ*, 539, 273
- Dmitruk, P. & Gomez, D. O. 1997, *ApJ*, 484, L83.
- Dmitruk, P. & Gómez, D. O. 1999, *ApJ*, 527, L63
- Doyle, J. G., Teriaca, L., & Banerjee, D. 2000, *A&A*, 356, 335
- Griffiths, N. W., Fisher, G. H., Woods, D. T., & Siegmund, O. H. W. 1999, *ApJ*, 512, 992
- Heyvaerts, J. & Priest, E. R. 1992, *ApJ*, 390, 297.
- Inverarity, G. W. & Priest, E. R. 1995, *A&A*, 296, 395.
- Inverarity, G. W., Priest, E. R., & Heyvaerts, J. 1995, *A&A*, 293, 913.
- Kuin, N. P. M. & Martens, P. C. H. 1982, *A&A*, 108, L1.
- Mariska, J. T. 1992, *The Solar Transition Region*, Cambridge Astrophysics Series, Cambridge University Press, Cambridge, United Kingdom
- Mariska, J. T., Feldman, U., & Doschek, G. A. 1978, *ApJ*, 226, 698
- Martens, P. C. H. 1981, *A&A*, 102, 156.
- Mason, H. E., Young, P. R., Pike, C. D., Harrison, R. A., Fludra, A., Bromage, B. J. I., & del Zanna, G. 1997, *Sol. Phys.*, 170, 143
- Matthaeus, W. H., Zank, G. P., Oughton, S., Mullan, D. J., & Dmitruk, P. 1999, *ApJ*, 523, L93.

McClymont, A. N. & Canfield, R. C. 1983, *ApJ*, 265, 497.

O’Shea, E., Gallagher, P. T., Mathioudakis, M., Phillips, K. J. H., Keenan, F. P., & Katsiyannis, A. C. 2000, *A&A*, 358, 741

Oughton, S., Matthaëus, W. H., Dmitruk, P., Milano, L. J., Zank, G. P., & Mullan, D. J. 2001, *ApJ*, 551, 565.

Raymond, J. C. & Doyle, J. G. 1981, *ApJ*, 247, 686

Rosner, R., Tucker, W. H., & Vaiana, G. S. 1978, *ApJ*, 220, 643

Schrijver, C. J. & Aschwanden, M. J. 2002, *ApJ*, 566, 1147.

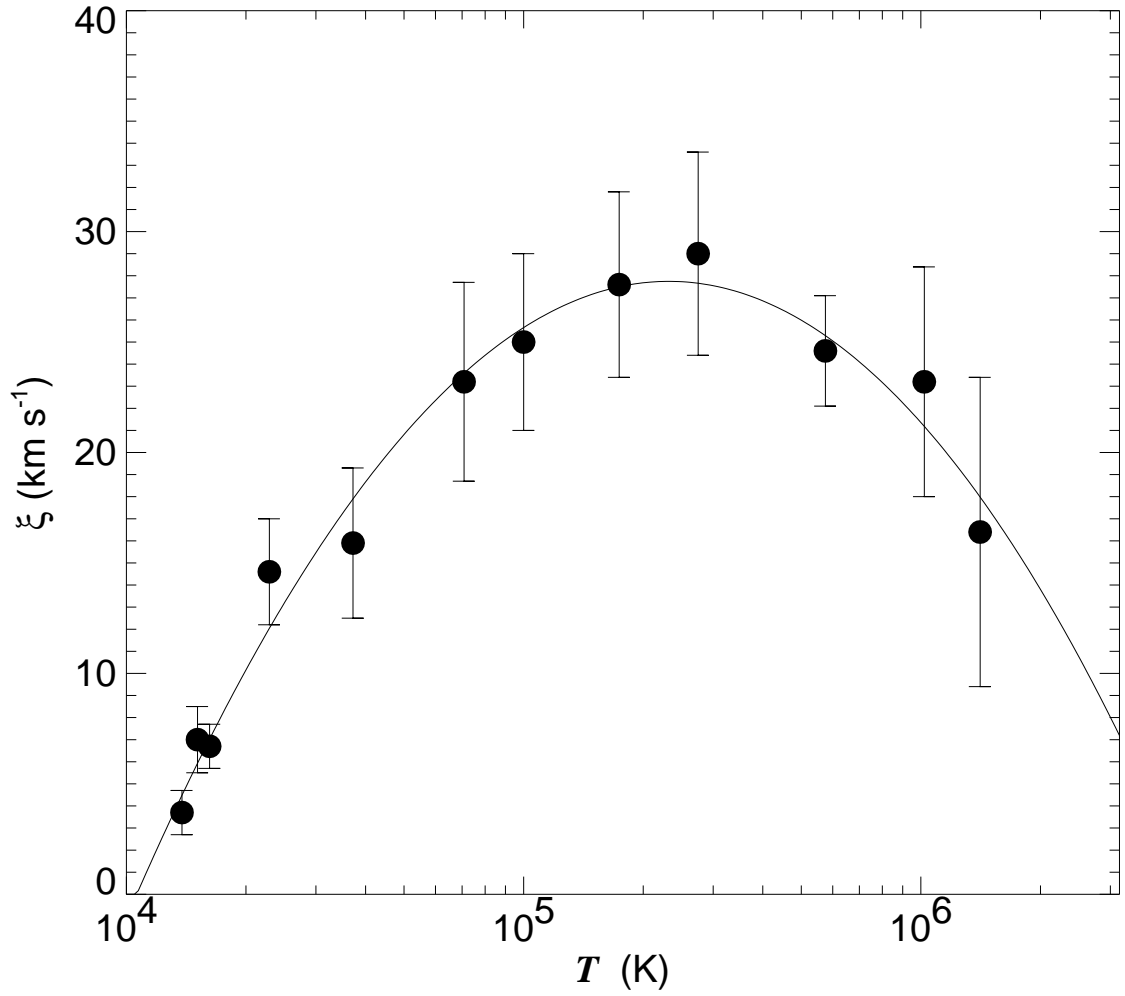


Fig. 1.— The observed non-thermal velocity in the transition region and corona of the quiet Sun. Adapted from Chae et al. (1998a).

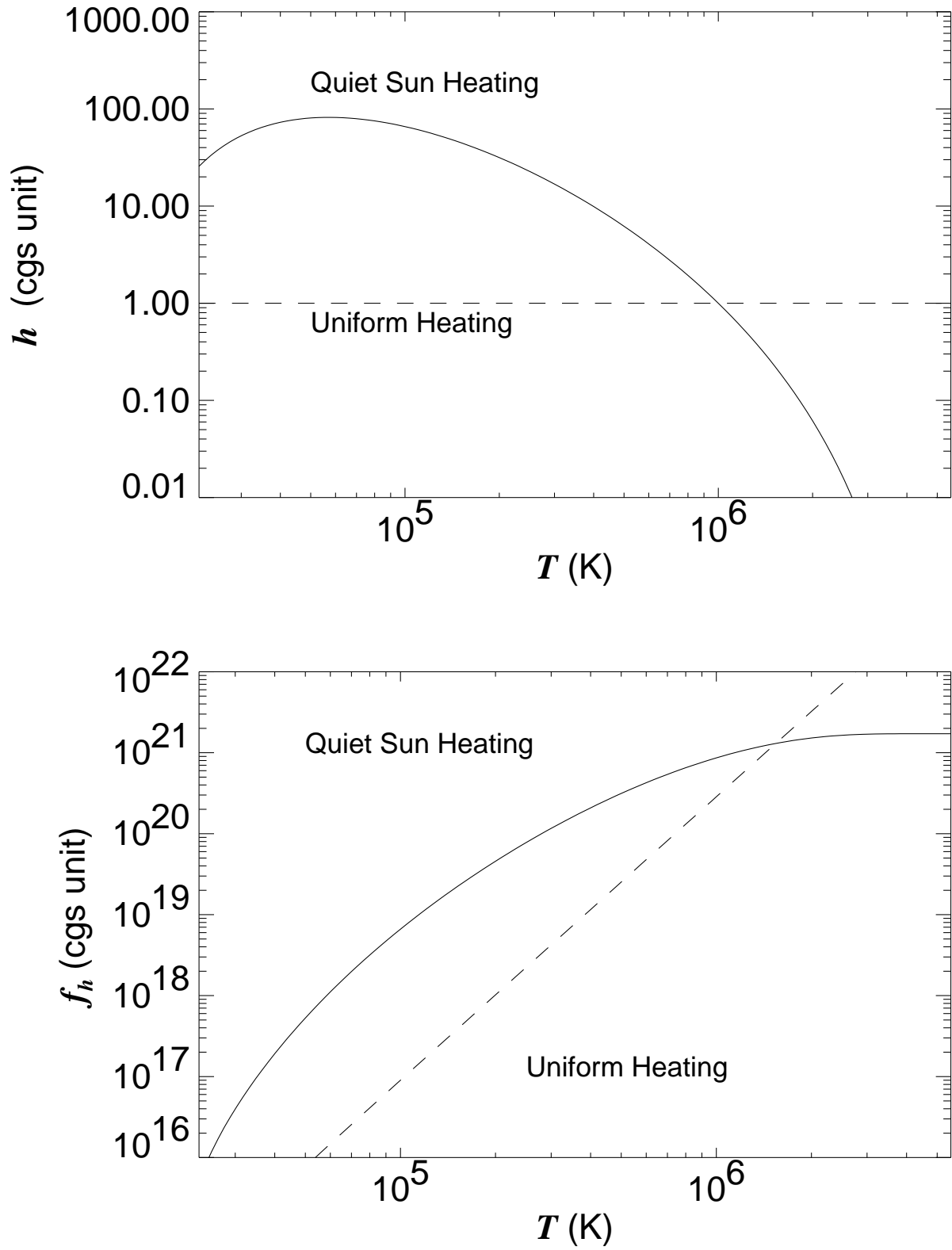


Fig. 2.— The  $h$  and  $f_h$  functions related to heating rates.

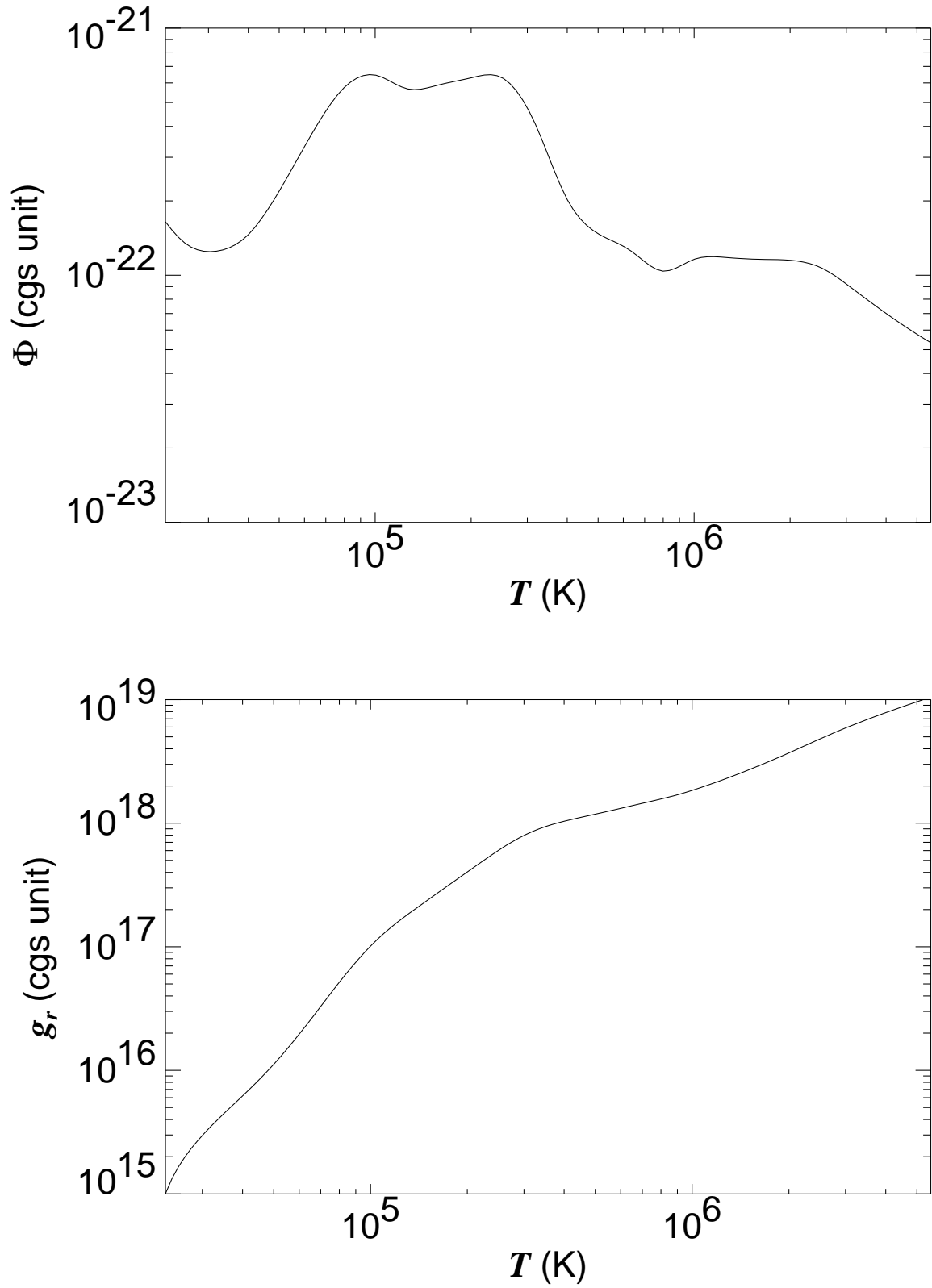


Fig. 3.— The  $\Phi$  and  $g_r$  functions related to radiative cooling.

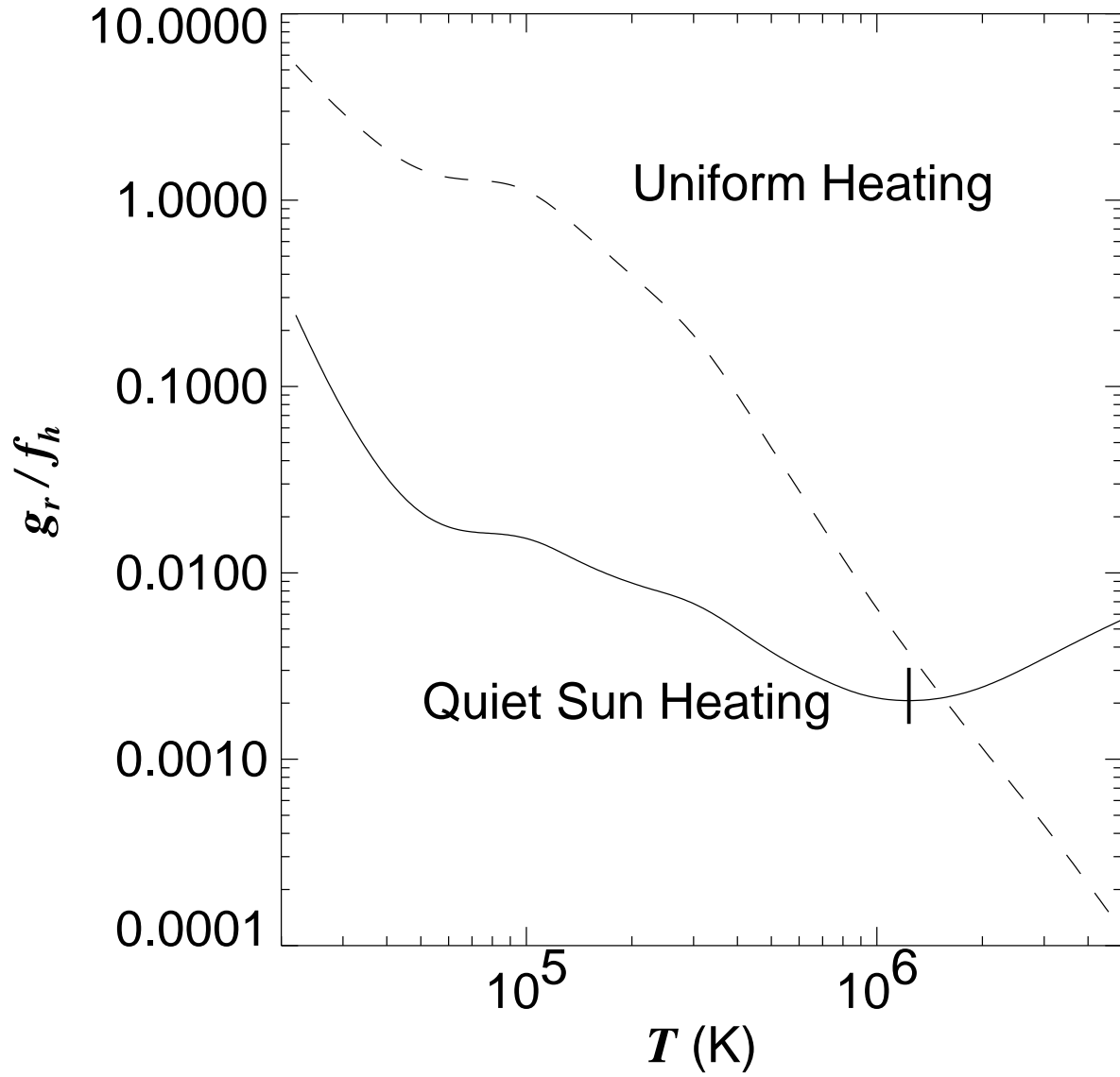


Fig. 4.— The functions  $g_r/f_h$  for the cases of uniform heating and non-uniform quiet Sun heating.

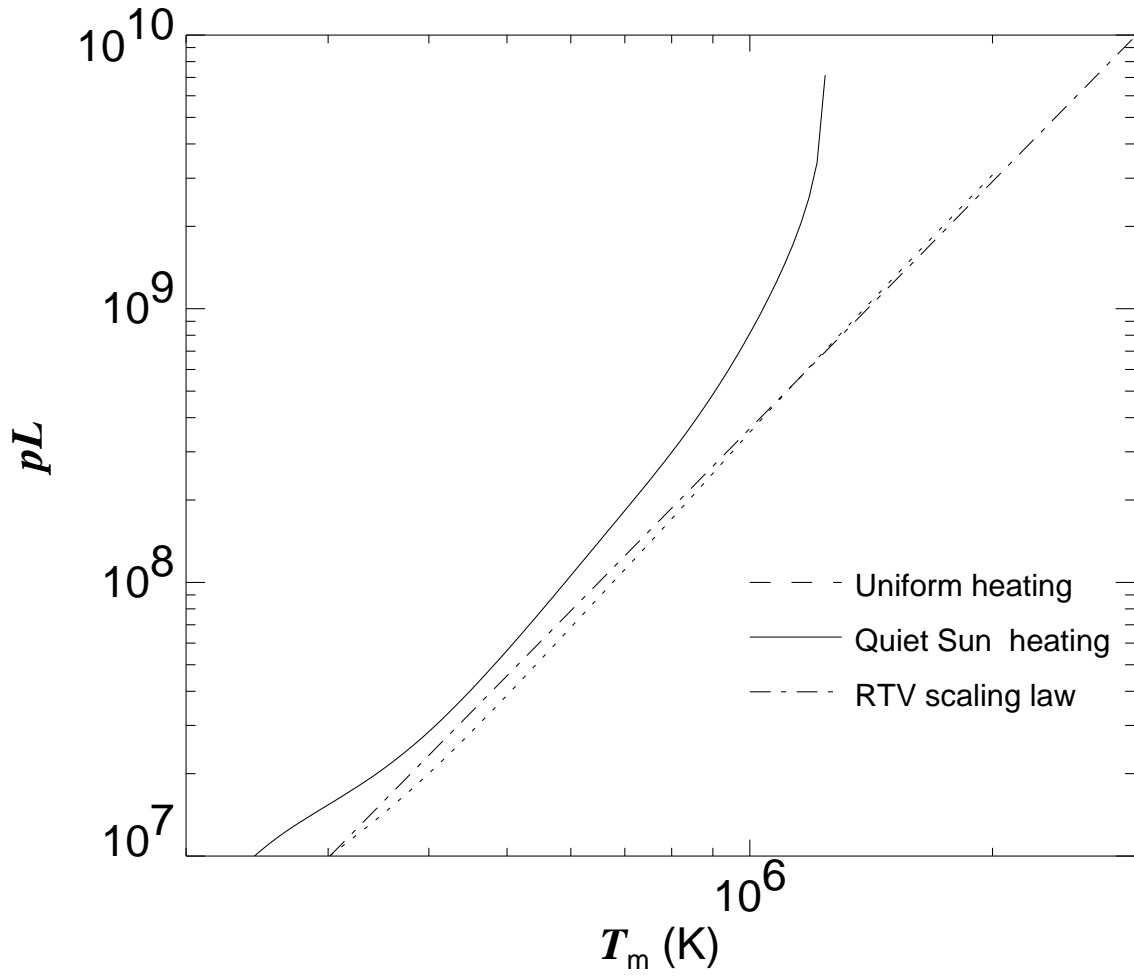


Fig. 5.— The scaling laws of  $pL$ .

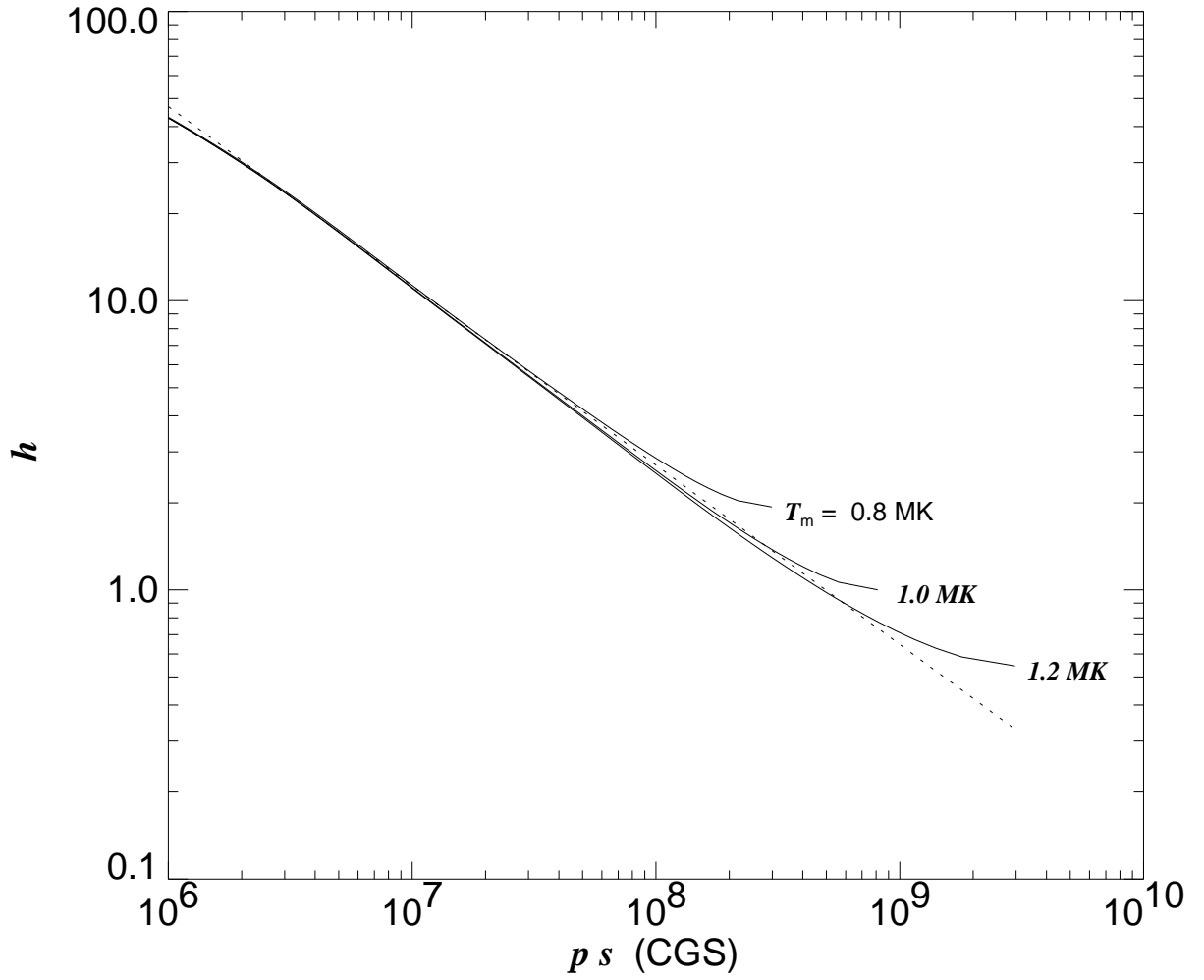


Fig. 6.— Heating rates as functions of arc length along the loops. The dotted curve is the analytic fit as presented in Equation 23.

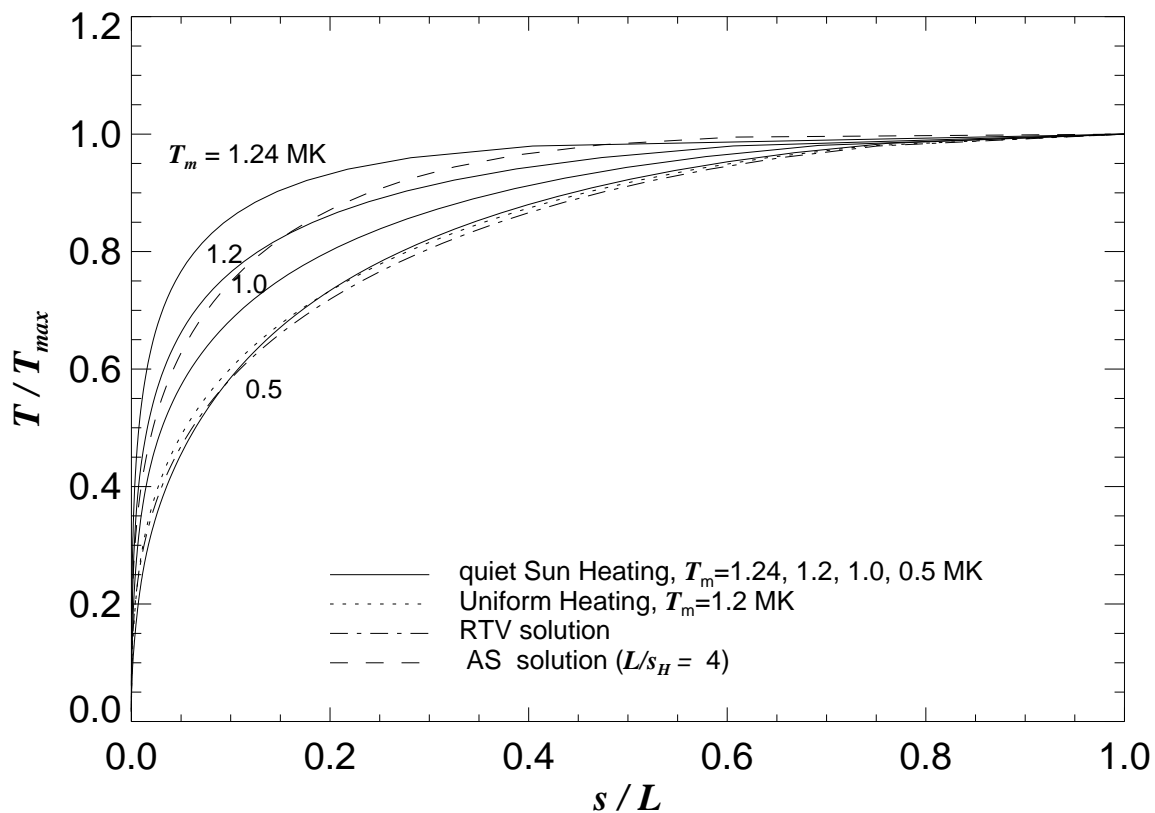


Fig. 7.— Temperature variations along the quiet Sun loops non-uniformly heated by MHD turbulence. The dashed curve represents an analytical solution obtained by Aschwanden and Schrijver (2002) in the case of  $L/s_H = 4$ .

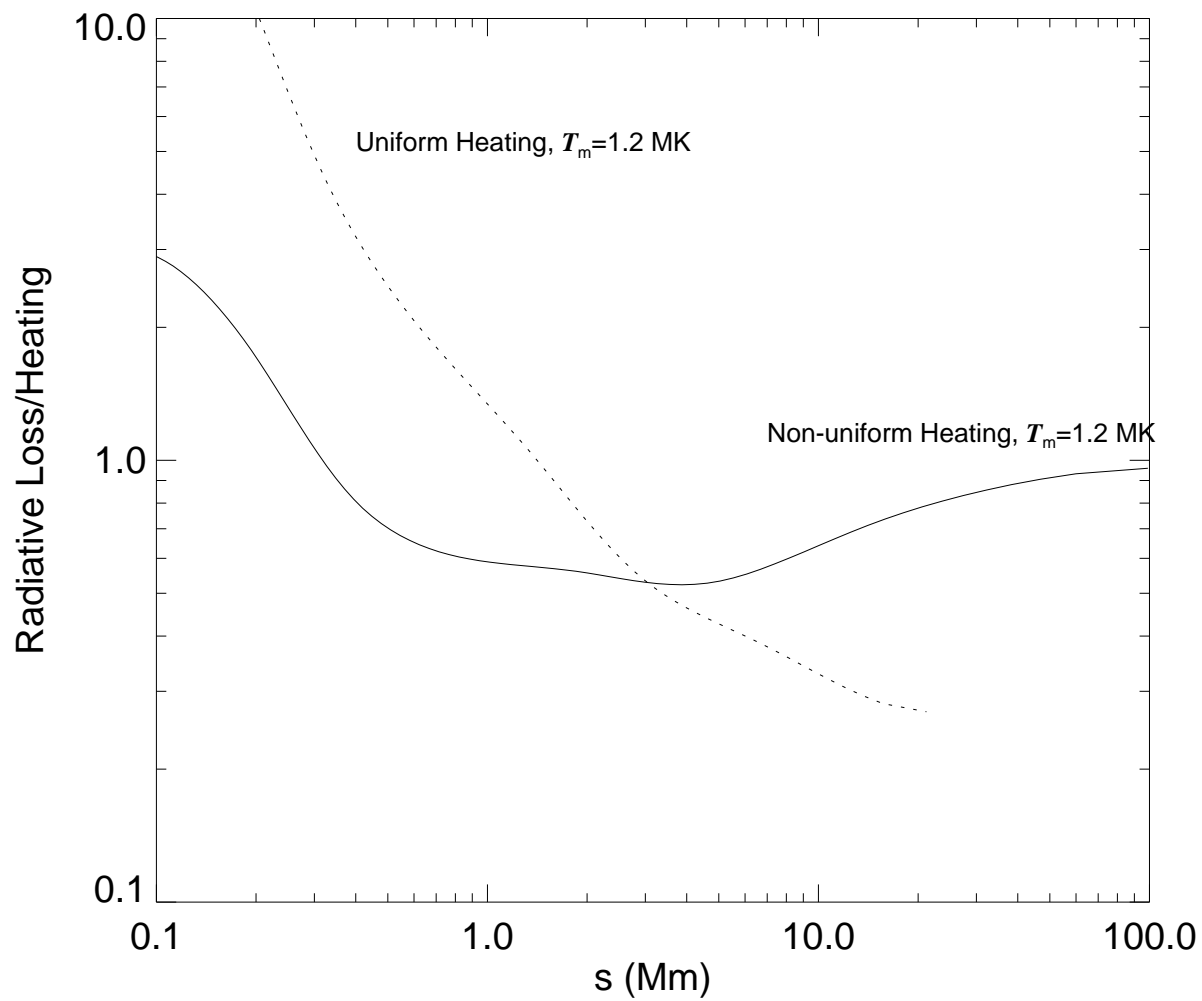


Fig. 8.— The ratio of radiative loss rate to heating rate.

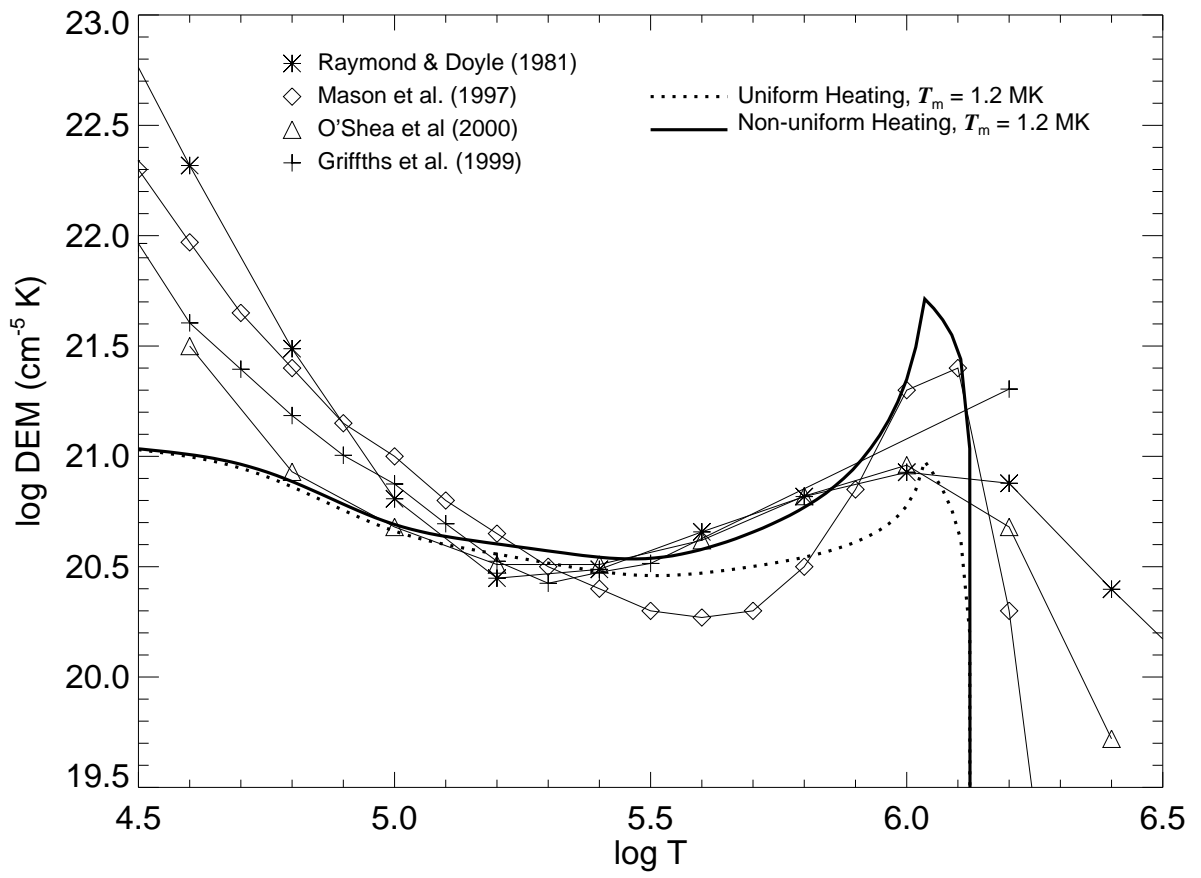


Fig. 9.— Differential emission measures.

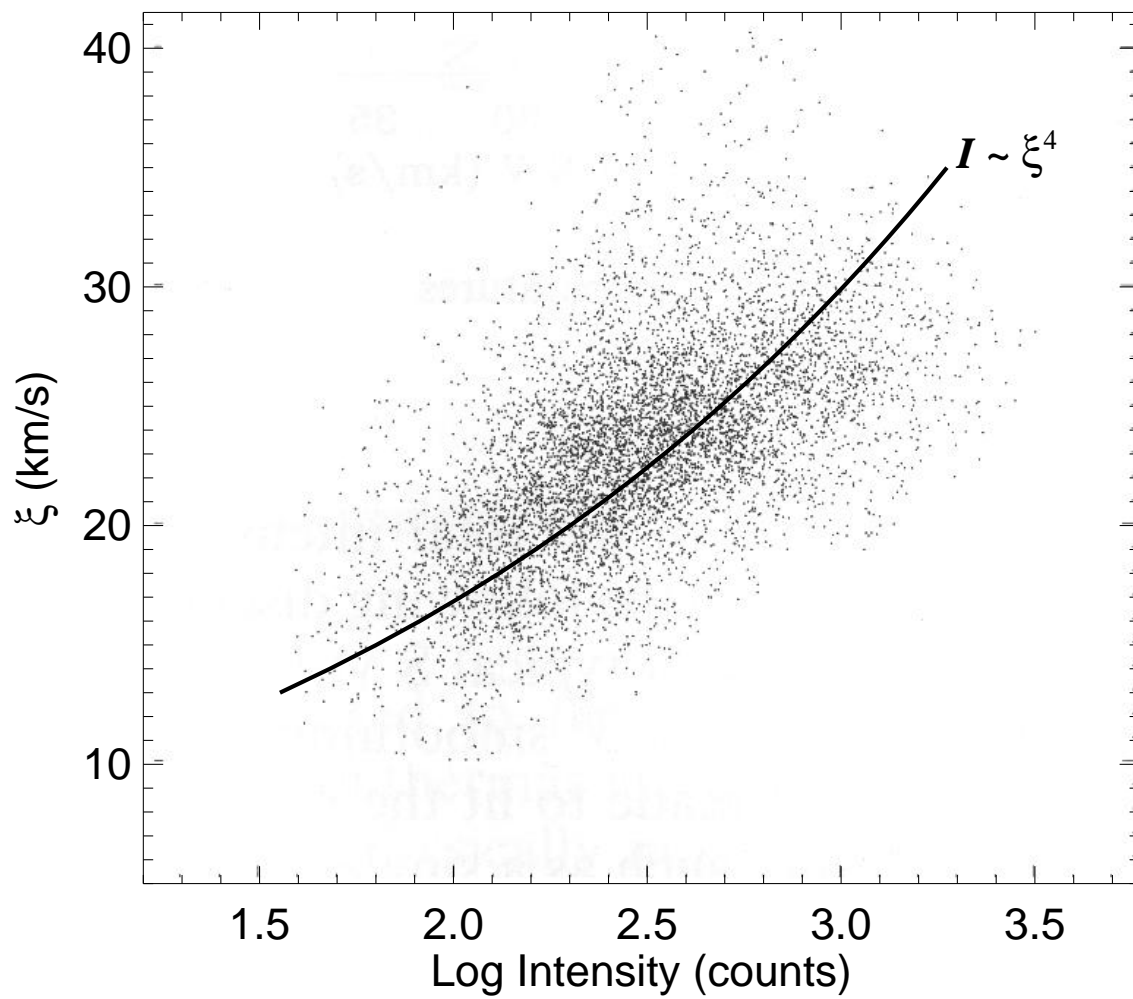


Fig. 10.— The scatter plot of non-thermal velocity versus the Si IV  $\lambda 1401$  line intensity in the quiet Sun reproduced from Chae et al. (1998a).